Applied Catalysis B: Environmental 148–149 (2014) 250–257

Contents lists available at ScienceDirect

Applied Catalysis B: Environmental

journal homepage: www.elsevier.com/locate/apcatb

Evaluating the sensitizing effect on the photocatalytic decoloration of dyes using anatase-TiO_2

Yu-Cheng Hsiao[a], Tsai-Fang Wu[a,b], Yu-Sheng Wang[a], Chi-Chang Hu[a,*], Chihpin Huang[b]

[a] Department of Chemical Engineering, National Tsing Hua University, 101, Section 2, Kuang-Fu Road, Hsin-Chu 30013, Taiwan
[b] Institute of Environmental Engineering, National Chiao Tung University, 1001 University Road, Hsin-Chu 30010, Taiwan

ARTICLE INFO

Article history:
Received 4 September 2013
Received in revised form 8 November 2013
Accepted 10 November 2013
Available online 16 November 2013

Keywords:
Photocatalysis
Dye-sensitizing effect
Titanium dioxide
Dye decoloration
Photocurrent–voltage curve

ABSTRACT

This work tries to clarify the contribution of the dye-sensitizing effect on the photocatalytic decoloration of dyes dissolved in aqueous media using an anatase TiO_2 (A-TiO_2) photocatalyst. The photocurrent-voltage (*J–V*) curves of a typical dye-sensitized solar cell (DSSC) with the A-TiO_2 photoanodes adsorbed with various dyes, including methylene blue (MB), orange G (OG), rhodamine B (RhB), metanil yellow (MY), acid black 24 (AB24), and N719, are employed to demonstrate the sensitizing characteristics of dyes on A-TiO_2. Unlike RhB, the MB, OG, MY, and AB24 cannot work as the photo-sensitizer on A-TiO_2 from the *J–V* curves of DSSCs, reasonably due to the unmatched band position between dyes and A-TiO_2. In the photocatalytic decoloration test of these dyes on A-TiO_2 in aqueous media, dye adsorption onto A-TiO_2 becomes the key factors affecting the photocatalytic decoloration rate because the generation of oxidants species (e.g., O_2^{-}•, OH• or photo-excited holes) occurs on the A-TiO_2 surface. The contribution of dye-sensitizing on the photocatalytic decoloration of RhB is negligible since the dye-sensitizing/electron-injection/dye-regeneration cycle cannot be completed in the degradation media while adsorbed RhB molecules are unstable when few photo-generated electrons have been injected into the conduction band of A-TiO_2, probably leading to the decomposition of RhB.

© 2013 Elsevier B.V. All rights reserved.

1. Introduction

The photo-electrochemical water splitting in the TiO_2//Pt system in the 1960s signalled the start of extensive research efforts in the semiconductor-based photocatalysis [1]. Among all photocatalysts, TiO_2 is widely proposed to be utilized in various applications, such as air purification [2], water purification [2–4], self-cleaning surfaces [1], antibacterial application [5,6], etc. due to its interesting photo-induced physicochemical properties, chemical and optical stability, non-toxicity, and low cost [1,7]. In fact, photocatalytic degradation of pollutants on TiO_2 has been recognized as one of the advanced oxidation processes (AOPs) for wastewater treatments, which usually employ hydroxyl radicals (OH•) or other strong oxidants to effectively remove or decompose organic compounds [1]. However, due to the wide band gap (3.2 and 3.0 eV for anatase and rutile TiO_2, respectively), the electron/hole pairs are necessarily photo-excited by the UV-light irradiation. Hence, how to effectively utilize solar light illumination on TiO_2 and other photocatalysts becomes a subject of intense research in photocatalysis, which has been reviewed in the literature [5,8,9].

One of the interesting methods which enhance the function of TiO_2 under the solar light irradiation is the usage of photo-sensitizers, such as dyes and quantum dots, having been employed in the sensitized-based solar cells [10] and water purification [11,12]. The photo-sensitized mechanism of the dye-adsorbed TiO_2 under the visible (Vis) light illumination can be simply expressed as follow: (1) the adsorbed dye is effectively excited to generate the electron/hole pair by the light illumination because of its narrower band gap in comparison with TiO_2 and (2) the photo-excited electrons are injected from the lowest unoccupied molecular orbital (LUMO) of adsorbed dyes into the conduction band (CB) of TiO_2 [10–13]. However, due to the 4–5% ultraviolet (UV) light in the solar light illuminated on the planet, certain UV photons can be directly absorbed by TiO_2 to generate the electron/hole pairs for producing OH• and/or O_2^{-}• [14,15] which will oxidize dye and pollutants directly. Furthermore, in the dye-sensitizing process, the highly reactive OH• has been proposed to be mainly produced by the photo-excited electrons, injected from the adsorbed dye molecules, on the conduction band of TiO_2 [16,17]. Thus, this process facilitated the Vis-light-driven OH• generation on TiO_2 for photocatalytic degradation of organics. However, some issues have to be considered in using the above TiO_2 adsorbed with photo-sensitizers. For example, in the dye-sensitized solar cells (DSSCs), besides the two steps proposed previously, an additional reaction between the adsorbed, positively charged dye molecules and the redox mediator

* Corresponding author. Tel.: +886 3 5736027; fax: +886 3 5736027.
E-mail address: cchu@che.nthu.edu.tw (C.-C. Hu).

0926-3373/$ – see front matter © 2013 Elsevier B.V. All rights reserved.
http://dx.doi.org/10.1016/j.apcatb.2013.11.014

(e.g., I^- of the I_3^-/I^- couple) completes the regeneration of dye molecules for the next dye-sensitization process. This regeneration step is prohibited by the absence of suitable redox mediators in the pollutant media, interrupting the next dye-sensitization process in the photocatalytic degradation mechanism. Therefore, in the photocatalytic degradation process, the adsorbed, positively charged dye is regarded as an organic ion radical which is highly reactive and should decompose spontaneously into other forms which will be decomposed by the hydroxyl radicals (OH•) or $O_2^{-\bullet}$ generated on the TiO_2 surface [11,12]. The second concern is the adsorption and coverage of dyes on the TiO_2 surface in the pollutant media because only the photo-excited electrons on the adsorbed dyes can be injected into the conduction band of TiO_2 without considering the possibly unmatched band position between dyes and TiO_2. The third issue is the variation in the $O_2^{-\bullet}$ or OH• generation rate on the TiO_2 surface via the electrons on the conduction band of TiO_2 because of the adsorption of photo-sensitizers.

In order to clarify the above concerns and the possible promotion in the photocatalytic activity of TiO_2 in the dye pollutant media, we employ a commercially available DSSC to test the band position matching between five typical dyes (i.e., methylene blue (MB), orange G (OG), rhodamine B (RhB), metanil yellow (MY), and acid black 24 (AB24)) and anatase-TiO_2 (A-TiO_2) since A-TiO_2 is generally shows relatively high reactivity and chemical stability under UV light excitation for water and air purifications, photocatalysts, and so on [2–4], further emphasizing its practical importance. Then, the photocatalytic decoloration of these dyes dissolved in the aqueous media on A-TiO_2 is compared to emphasize the importance of dye adsorption on A-TiO_2 in the photocatalytic degradation of dyes and organics. The above important concepts in photocatalysis, never reported before, will be clarified in this work.

2. Experimental details

2.1. Preparation of dye-sensitized solar cells

The photo-anode and counter electrode substrates of the DSSCs were the transparent, conductive F-doped SnO_2 (FTO) glass. A-TiO_2 films were coated with a commercially available A-TiO_2 slurry (Eversolar® P-200, Everlight Chemical Co., Taiwan) using the screen printing method. The TiO_2-coated FTO electrode was calcinated at 500 °C for 30 min to generate the mesopores within the TiO_2 film. The TiO_2 photo-anode was soaked with a binary solvent mixture of equal-volume acetonitrile and tert-butanol (Scharlau), which contains 3×10^{-4} M dye, including MB (Sigma-Aldrich), OG (Sigma-Aldrich), RhB (Sigma-Aldrich), MY (Alfa-Aesar), AB24 (AK scientific), and N719 ruthenium-based dye (Solaronix SA, Switzerland), for 24 h to achieve the saturated adsorption of dye on the TiO_2 photo-anode. The TiO_2 photo-anode soaked with dye were rinsed with anhydrous ethanol and dried in air. The photosensitive area and thickness of the TiO_2 film on the photo-anode was 0.25 cm^2 and 10 μm, respectively. The semi-transparent Pt-coated FTO electrode (with 75% transparency) working as the counter electrode was prepared by sputtering. The TiO_2 photo-anode and the Pt-coated FTO electrode were assembled into a solar cell with a spacer (a Surlyn film, SX1170–60, Solaronix SA, Switzerland). The cell gap was fixed at about 25 μm. The 3-MPN (3-methoxypropionitrile, Eversolar® EL-200, Everlight Chemical Co., Taiwan) electrolyte, containing 0.6 M tetrabutylammonium iodide, 0.1 M iodine, and 0.5 M *tert*-(butyl pyridine), was injected into the cell to form a simple package of DSSCs.

2.2. Photo-sensitization and dye-sensitization measurements

The photocurrent-voltage (*J–V*) curves were measured by a computer-controlled digital source meter (Keithley, model 2400) under the simulated solar irradiation (PEC-L15, Peccell), in which the light intensity was set at 100 mW cm^{-2} (AM1.5). In addition, the simulated solar light with UV-cut off filter (<400 nm) was used as the Vis-light source for measuring the purely dye-sensitized *J–V* curves of the DSSCs containing various dyes. From the *J–V* curves, the photo-electrochemical parameters, such as short-circuit photocurrent density (J_{SC}), open circuit voltage (V_{OC}), fill factor (*FF*), and energy conversion efficiency (η), can be obtained. The fill factor was defined as Eq. (1) [18,19]:

$$FF = \frac{(J_{max} V_{max})}{(V_{oc} J_{sc})} \quad (1)$$

where J_{max} and V_{max} are the photocurrent density and voltage obtained at the maximum power output. The energy conversion efficiency is defined as Eq. (2):

$$\eta(\%) = \frac{P_{out}}{P_{in}} \times 100\% = \frac{J_{max} V_{max}}{P_{in}} \times 100\% = \frac{(J_{sc}\, V_{oc}\, FF)}{P_{in}} \times 100\% \quad (2)$$

where P_{in} indicates the power input of the light intensity.

2.3. Photo-electrochemical and photocatalytic decoloration measurements in aqueous media

The photocurrent density against potential (*i–V*) characteristics were conducted in aqueous media by an electrochemical analyser system CHI 1127A (CH Instruments, USA) using linear sweep voltammetry (LSV) under a two-electrode mode where A-TiO_2-coated FTO electrode and *Pt* wire acted as the anode and cathode, respectively. The *i–V* responses were measured under illumination of the Vis-light source with the light intensity equal to 78 mW cm^{-2} in the repeated light-on/-off test. The aqueous media for the *i–V* measurement was a 0.1 M KCl solution without and with 10 ppm dyes including MB, OG, RhB, MY, or AB24.

In the photocatalytic decoloration test of MB, OG, RhB, MY, and AB24, the A-TiO_2 photo-anodes were immersed in a 20-mL solution containing 10 mg L^{-1} dye under stirring in darkness for 40 min in order to achieve the saturation of dye adsorption. The photocatalytic decoloration was conducted under the simulated solar light illumination with the light intensity equal to 100 mW cm^{-2} (AM 1.5) and Vis-light irradiation with the light intensity equal to 78 mW cm^{-2}. The variation in MB, OG, RhB, MY, and AB24 concentrations was determined from the absorbance at 664, 478, 553, 435 and 571 nm by a UV–Vis spectrometer (SHIMADZU UV-2450) every 20 min. The photo-decoloration of dyes was conducted under the same condition of the photocatalytic decoloration test without A-TiO_2. N719 was not examined in the photocatalytic decoloration test because N719 is hardly dissolved in H_2O.

3. Results and discussion

3.1. Photo-sensitization and dye-sensitization analyses

There is a doubt that the LUMO of organic dyes and the CB of A-TiO_2 are matched each other in order to smoothen the photo-excited electron injection from the adsorbed dyes to A-TiO_2. If the LUMO of photo-sensitizers is significantly lower than the CB position of A-TiO_2, the photo-generated electrons cannot be effectively injected into A-TiO_2. As a result, such dyes cannot be used to promote the generation of highly reactive OH• and $O_2^{-\bullet}$ on A-TiO_2 for the photocatalytic degradation of organics. The above concern can be clarified by examining the photo-electrochemical responses of dye-adsorbed A-TiO_2 photo-anodes. In this work, the performance parameters (i.e., J_{SC}, V_{OC}, *FF*, and η) of a DSSC using the dyes of interest are employed as the index to evaluate the dye-adsorbed A-TiO_2 photo-anodes. In order to confirm the acceptable performances of the DSSC prepared in this work in the solar energy conversion,

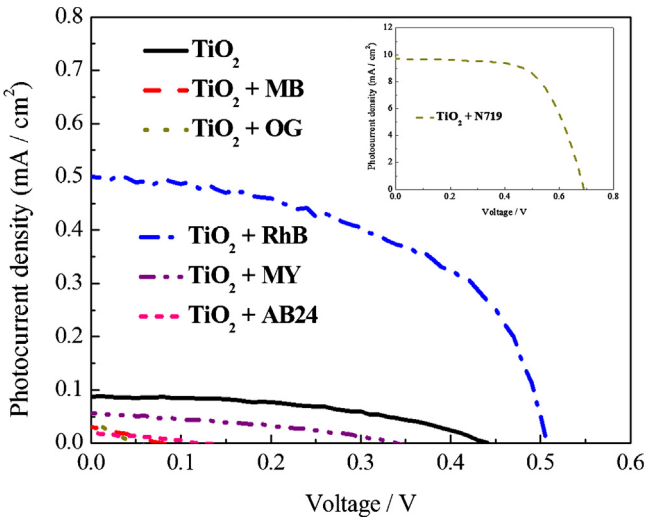

Fig. 1. The *J–V* (photocurrent density against cell voltage) curves of the DSSC soaked with various dyes under the simulated solar irradiation (100 mW cm^{-2}, AM 1.5). Inset shows the typical *J–V* curve of a DSSC employing N719 as the sensitizer. (For interpretation of the references to color in this figure legend, the reader is referred to the web version of this article.)

the energy conversion efficiency of the DSSC with the N719 dye is determined, and its typical *J–V* curve is shown in the inset of Fig. 1. From this *J–V* curve, the performances of this DSSC are fairly good (i.e., J_{SC}, V_{OC}, *FF*, and η are equal to 9.830 mA cm^{-2}, 0.690 V, 0.640, and 4.346%, respectively). Accordingly, such a cell is typical for examining the photo-electrochemical characteristics of various dye-sensitized A-TiO_2 photo-anodes.

Fig. 1 shows the typical *J–V* characteristics of the DSSCs constructed with A-TiO_2 photo-anodes respectively adsorbed with MB, OG, RhB, MY, and AB24 under the 100 mW cm^{-2} simulated solar light irradiation. For a comparison purpose, the *J–V* curve measured from a solar cell with a bare A-TiO_2 photo-anode is also shown in this figure. From the *J–V* curves, the important photo-electrochemical parameters of J_{SC}, V_{OC}, *FF*, and η can be obtained, which are listed in Table 1. From Table 1, J_{SC} of the DSSC with a bare TiO_2 photo-anode is only 0.087 mA cm^{-2} because of the 4–5% of UV light in the simulated solar light. However, this photocurrent density is obviously higher than those from the cells with MB-, OG-, MY-, and AB24-adsorbed TiO_2 photo-anodes (i.e., 0.030, 0.042, 0.057 and 0.021 mA cm^{-2}, respectively). Clearly, the adsorption of MB, OG, MY, and AB24 on the A-TiO_2 photo-anodes only reduces the energy conversion performance (in all parameters; i.e., J_{SC}, V_{OC}, *FF* and η) of the resultant DSSCs. This result indicates that the LUMO positions of MB, OG, MY, and AB24 are significantly lower than the CB of A-TiO_2, leading to the ineffective injection of photo-excited electrons from these adsorbed dyes into A-TiO_2. In fact, the CB of A-TiO_2 is about −4.1 eV (*vs.* vacuum) [20,21] which is higher than the LUMO of MB (ca −4.25 eV (*vs.* vacuum)) [22], supporting the above statement. Moreover, A-TiO_2 on the dye-adsorbed photo-anodes should be shielded by the adsorbed dye molecules, thus, reducing the photocurrent density generated from A-TiO_2 due to the 4–5% UV light in the simulated solar light. As a result, the photovoltaic performances of a DSSC using MB, OG, MY, and AB24 as the sensitizer are worse than those of a DSSC without any dye.

Table 1
The results of photo-electrochemical parameters derived from the *J–V* curves of the DSSC soaked with various dyes under the simulated solar irradiation (100 mW cm^{-2}, AM 1.5).

Photo-anode	J_{SC} (mA cm^{-2})	V_{OC} (V)	*FF*	η (%)
TiO_2	0.087	0.44	0.465	0.018
MB-TiO_2	0.030	0.08	0.241	0.001
OG-TiO_2	0.042	0.05	0.239	0.001
RhB-TiO_2	0.500	0.51	0.524	0.133
MY-TiO_2	0.057	0.34	0.347	0.007
AB24-TiO_2	0.021	0.12	0.285	0.001
N719-TiO_2	9.830	0.69	0.640	4.346

Table 2
The photocurrent density (J_{SC}), background current density (J_{BG}, i.e., dark current), and open circuit voltage (V_{OC}) of the DSSC soaked with various dyes under the Vis-light irradiation (78 m W cm^{-2}).

Photo-anode	Visible light		Background	
	J_{SC} (mA cm^{-2})	V_{OC} (V)	J_{BG} (mA cm^{-2})	V_{OC} (V)
TiO_2	0.023	0.33	0.012	0.34
MB-TiO_2	0.024	0.07	0.010	0.08
OG-TiO_2	0.022	0.04	0.012	0.04
RhB-TiO_2	0.387	0.49	0.007	0.20
MY-TiO_2	0.020	0.25	0.012	0.29
AB24-TiO_2	0.013	0.11	0.010	0.13
N719-TiO_2	8.370	0.69	0.010	0.23

The DSSC with RhB as the sensitizer shows higher J_{SC}, V_{OC}, *FF*, and η than the one with a bare TiO_2 photo-anode, revealing that the LUMO of RhB is higher than the conduction band of A-TiO_2 [22]. Hence, the photo-excited electrons of RhB can be injected from the LUMO of this dye to the conduction band of A-TiO_2 to enhance the photo-energy conversion efficiency. On the other hand, the energy conversion efficiency of the N719-adsorbed DSSC is much higher than that of the RhB-adsorbed one because of two reasons. First, the electron injection rate from N719 to A-TiO_2 is expected to be much faster than that from RhB to A-TiO_2, probably due to the formation of the carboxylate bond between N719 and A-TiO_2 since the carboxylate bonds are considered a bridge for electron transmission [23]. Second, the band gap of N719 is smaller than that of RhB; as a result, more electrons can be excited by the simulated solar light irradiation when N719 is employed as the photo-sensitizer.

In order to circumvent the influences of the UV light on the generation of photo-excited electrons from A-TiO_2, a Vis-light source was employed in measuring the photovoltaic performances of the seven DSSCs examined in Fig. 1. The typical *J–V* curves are shown in Fig. 2 meanwhile the data of J_{SC}, V_{OC}, and background current density (J_{BG}) are compared in Table 2. From Fig. 2 and Table 2, several features have to be mentioned. First, the difference between the background current density (i.e., dark current) and J_{SC} on bare A-TiO_2, MB-adsorbed TiO_2, OG-adsorbed TiO_2 and MY-adsorbed TiO_2 photo-anodes under the Vis-light illumination are very similar. These results reveal the ineffective injection of photo-excited electrons from MB, OG, and MY, although these three dyes should be excited by the Vis-light illumination. Therefore, the photo-excited electrons cannot be transferred from the LUMO of these dyes into the conduction band of A-TiO_2, again revealing the unmatched band positions between the LUMO of both dyes and the conduction band of A-TiO_2. Second, the difference between the background current density (i.e., dark current) and J_{SC} on AB24-adsorbed TiO_2 photo-anodes under the Vis-light illumination is obviously lower than that on the bare A-TiO_2 photo-anode, suggesting a higher shielding effect of this dye. This phenomenon is attributable to the higher adsorption ability of AB24 on A-TiO_2 and its higher Vis-light absorption ability in comparison with the above three dyes (see below). Third, the difference between the J_{SC} and background current density on the RhB- and N719-adsorbed TiO_2 photo-anodes are obviously higher than that on the bare A-TiO_2, revealing that the photo-excited electrons of both dyes can be injected into the conduction band of A-TiO_2. Accordingly, in the photocatalytic degradation test, the decoloration rate and efficiency obtained in the RhB medium are expected to be higher than

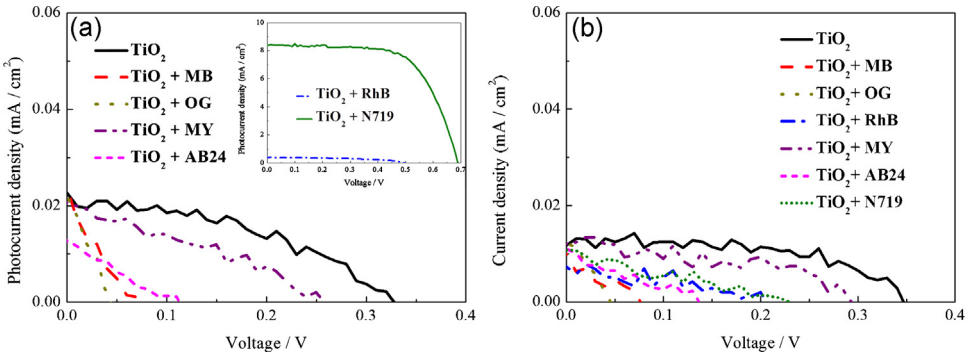

Fig. 2. The *J–V* (photocurrent density against cell voltage) curves of the DSSC soaked with various dyes under (a) Vis-light irradiation (78 mW cm^{-2}) and (b) dark (i.e., background current density or the so-called dark current). Inset in (a) shows the typical *J–V* curve of a DSSC employing RhB and N719 as the sensitizer. (For interpretation of the references to color in this figure legend, the reader is referred to the web version of this article.)

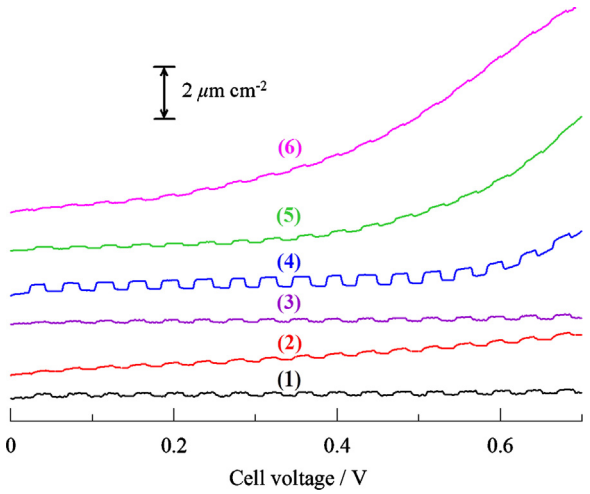

Fig. 3. The LSV curves of the A-TiO_2 photo-anode measured in (1) 0.1 M KCl, (2–6) with the addition of 10 ppm (2) methylene blue, (3) orange G, (4) rhodamine B, (5) metanil yellow, and (6) acid black 24 under the repeated Vis-light irradiation. (For interpretation of the references to color in this figure legend, the reader is referred to the web version of this article.)

that in the MB, OG, MY, and AB24 solutions because of the photo-sensitizing enhancement effect described in Introduction.

In order to correlate the *J–V* responses of DSSCs soaked with various dyes to the photocatalytic decoloration of dyes on A-TiO_2, the polarization curves of an A-TiO_2 photo-anode in the solution containing 0.1 M KCl and 10 ppm dyes under the repeated light-on/-off cycles of the visible light were measured. Typical LSV curves measured at 10 mV s^{-1} are shown in Fig. 3 meanwhile the LSV curve measured in 0.1 M KCl without any dye (curve 1) is shown in the same figure for a comparison purpose. In addition, the photocurrent densities measured at 0.4 V for various dyes are shown in Table 3.

From curve 1, the background current density is gradually increased with the positive shift in the cell voltage (E_{cell}) meanwhile extremely low current fluctuation (ca. 160 nA cm^{-2}) is found. The latter result reveals that a few electrons in the valence band of A-TiO_2 have been excited by the simulated solar light with UV-cut off filter (<400 nm), probably due to the presence of minor amount of UV-light. Similar responses have been found for the solutions containing MB, OG, MY, and AB24. However, from Table 3, MB, OG, MY, and AB24 cannot act as a photo-sensitizer on A-TiO_2, which reduce the light intensity because of the shielding effect. Hence, the photocurrent densities obtained at 0.4 V in the KCl solutions containing these four dyes are lower than that in the blank electrolyte (0.1 M KCl). Note the much larger photocurrent density measured from the KCl + RhB solution, attributable to the photo-sensitizing effect of RhB repeatedly excited by the light source. Accordingly, the adsorbed RhB molecules on A-TiO_2 can work as a photo-sensitizer to produce photo-excited electrons which are effectively injected from the LUMO of RhB to the CB of A-TiO_2 under the Vis-light illumination. Also note that direct oxidation of dyes on A-TiO_2 in the relatively positive potential region should occur, leading to the obvious increase in the anodic current with the increase in the cell voltage (e.g., see curve 3 at E_{cell} > 0.6 V, curve 4 at E_{cell} > 0.6 V, and curve 5 at E_{cell} > 0.3 V). However, it is not easy to judge the onset potential for the direct oxidation of MB and AB24 from their corresponding LSV curves.

Based on all the above results and discussion, schematic illustration of the photo-sensitizing responses and the possible enhancement in the photocatalytic degradation reaction for various dyes investigated in this work is shown in Fig. 4. The band gaps of all dyes employed here are lower than that of A-TiO_2, which are Vis-light-sensitive. Accordingly, the photo-excited electrons can be generated on all dyes by means of the solar light illumination. However, only the photo-excited electrons on the LUMO of RhB and N719 can be effectively injected into the conduction band of A-TiO_2 since the LUMOs of RhB and N719 are higher than the conduction band of A-TiO_2. Moreover, due to the 4–5% UV light in the solar light, bare A-TiO_2 can be excited by the UV light irradiation to generate the electron/hole pairs. These electrons on the conduction band of A-TiO_2 are possibly donated to the oxygen molecules adsorbed on A-TiO_2 to generate $O_2^{-\bullet}$. Thus, hydroxyl radicals (OH•) or other strong oxidative species will be formed near the A-TiO_2 surface by all the photo-excited electrons and the holes on A-TiO_2, leading to the decoloration of dyes. Moreover, adsorbed dyes may be decolorized by the photo-excited holes through means of direct oxidation (i.e., dyes act as the hole scavenger), further promoting the decoloration efficiency. On the other hand, for the wastewater containing MB, OG, MY, or AB24, the photo-excited electrons generated from the dyes cannot be effectively injected into the conduction band of A-TiO_2 because of unmatched band position between LUMO of dyes and CB of A-TiO_2. Accordingly, these dyes only can be decolorized by the strong oxidative species ($O_2^{-\bullet}$,OH•

Table 3
The photocurrent density of an A-TiO_2 photo-anode measured at 0.4 V in the solution containing 0.1 M KCl and 10 ppm dyes under the repeated light-on/-off cycles of the Vis-light (78 mW cm^{-2}).

Electrolyte	Photocurrent density at 0.4 V (nA cm^{-2})
KCl	161.06
KCl + MB	135.50
KCl + OG	148.27
KCl + RhB	451.73
KCl + MY	140.11
KCl + AB24	95.73

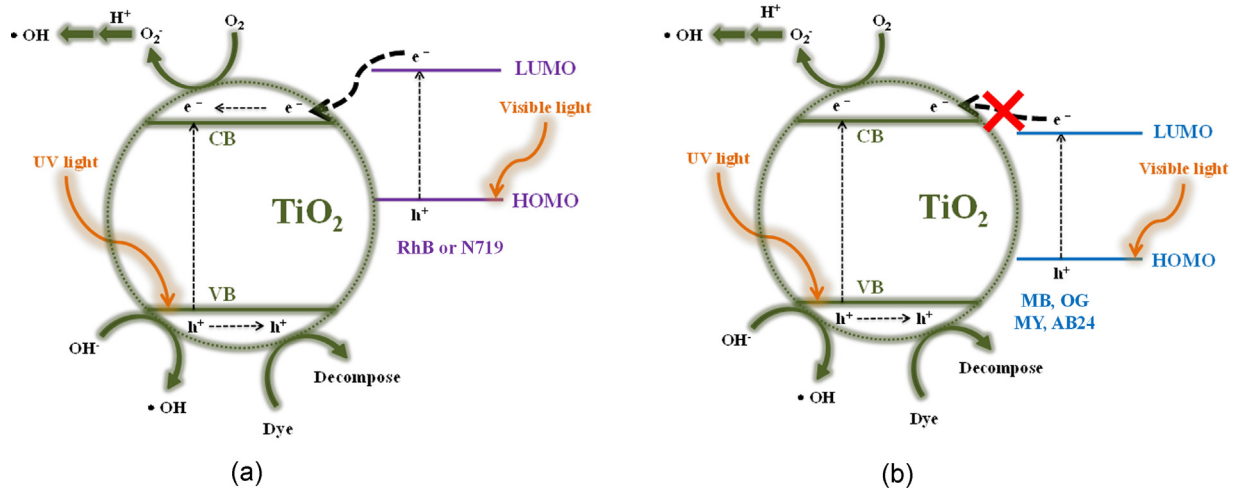

Fig. 4. Schematic mechanisms illustrate (a) matched and (b) unmatched band position between LUMO of dyes and CB of A-TiO_2. The enhanced photo-sensitizing current and the generation of highly oxidative species on the A-TiO_2 surface are expected to occur via mechanism (a).

or photo-excited holes) on A-TiO_2 itself. In other words, there is no possibility to run the photo-sensitizing enhancement route in the photocatalytic degradation of dyes when MB, OG, MY or AB24 are the organics to be decolorized. Furthermore, the shielding effect due to dye adsorption will reduce the generation of photo-excited electron/hole pairs on A-TiO_2, reducing the formation of strong oxidants for the photocatalytic degradation of pollutants.

3.2. Photocatalytic decoloration and photo-decoloration of dyes

Based on the results and discussion in the previous section, the photocatalytic decoloration of RhB by A-TiO_2 might be enhanced via the photo-sensitizing enhancement route. In order to verify the contribution from the photo-sensitizing enhancement route in the photocatalytic degradation of RhB, the A-TiO_2 photo-anode was employed to decolorize the wastewater containing MB, OG, RhB, MY, and AB24. The concentration of dyes in all solutions is fixed (10 mg L^{-1}) meanwhile the typical UV–Vis spectra of the test solutions decolorized by the A-TiO_2 photo-anode irradiated with a simulated solar light (100 mW cm^{-2}, AM 1.5) for 0–100 min are shown in Fig. 5. Note that during the initial 40 min, the light source was turned off; this period was used to reach saturation of dye adsorption on the A-TiO_2 photo-anode immerged in the dye solution. The adsorption of all dyes has been confirmed to be saturated in the above 40-min adsorption step since the UV–Vis spectra of every dye-containing solution approximately overlap in the whole wavelength region when the adsorption time is equal to/longer than 30 min (not shown here). When the light source was turned on at t = 40 min, decoloration of dyes occurred steadily, leading to the steady decrease in the absorbance of the UV–Vis spectra. Note that after the 40-min adsorption step, the absorbance at 664, 478, 553, 435, and 571 nm was employed to represent the initial concentration (i.e., C_0) of dyes in the photocatalytic decoloration test for the MB-, OG-, RhB-, MY-, and AB24-containing solutions, respectively.

Fig. 6(a) and (b) respectively shows the variation in C/C_0 of various dyes with respect to the decoloration time for photo-decoloration and photocatalytic decoloration by the A-TiO_2 photo-anode under the simulated solar light irradiation. From Fig. 6(a), only MB and AB24 were significantly decolorized by the simulated solar light (i.e., photo-decomposition of MB and AB24), revealing the photochemical stability of OG, RhB, and MY. From Fig. 6(b), on the other hand, all dyes were significantly decolorized when the A-TiO_2 photo-anodes were immersed in the dye solutions, revealing the photocatalytic decoloration of A-TiO_2. In addition, the order of dyes with respect to decreasing the decoloration percentage by means of the photocatalytic route under the simulated solar light is: MB (10.34%) > AB24 (7.04%) > RhB (5.72%) > OG (2.32%) ≈ MY (2.05%; see Table 4). This order, however, is different from the expectation from the photo-electrochemical energy conversion data and the polarization results shown in Fig. 3 and Table 3. Interestingly, the rates of MB and AB24 decoloration are obviously faster than that of RhB although the latter dye has been confirmed to be a photo-sensitizer for promoting the photocurrent density and enlarging the open circuit voltage of a DSSC in Fig. 1. From Table 1, J_{SC} from the RhB-based DSSC is about 17 times and 24 times of that from the MB-based and AB24-based DSSCs. Thus, the photocatalytic decoloration rate of the RhB solution is expected to be 17 times and 24 times of the MB- and AB24-containing media if the mechanism proposed in Fig. 4(a) is the main route responsible for the RhB decoloration. However, opposite results are obtained, indicating that there is another key factor determining the photocatalytic decoloration rate of dyes on A-TiO_2.

In this work, 1 mg A-TiO_2 powders were dispersed in a 20-mL solution containing 10 mg L^{-1} dye under stirring in darkness

Table 4
The photocatalytic decoloration and photo-decoloration percentages of MB, OG, RhB, MY, and AB24 by A-TiO_2 under the simulated solar light (100 mW cm^{-2}, AM 1.5) and Vis-light irradiation (78 mW cm^{-2}).

Dye	Simulated solar light		Visible light	
	Photo-decoloration (%)	Photocatalytic decoloration (%)	Photo-decoloration (%)	Photocatalytic decoloration (%)
MB	9.00	19.34	0.70	0.69
OG	0.00	2.32	0.00	0.00
RhB	0.00	5.72	0.00	0.19
MY	0.00	2.05	0.00	0.00
AB24	7.35	14.39	5.04	5.63

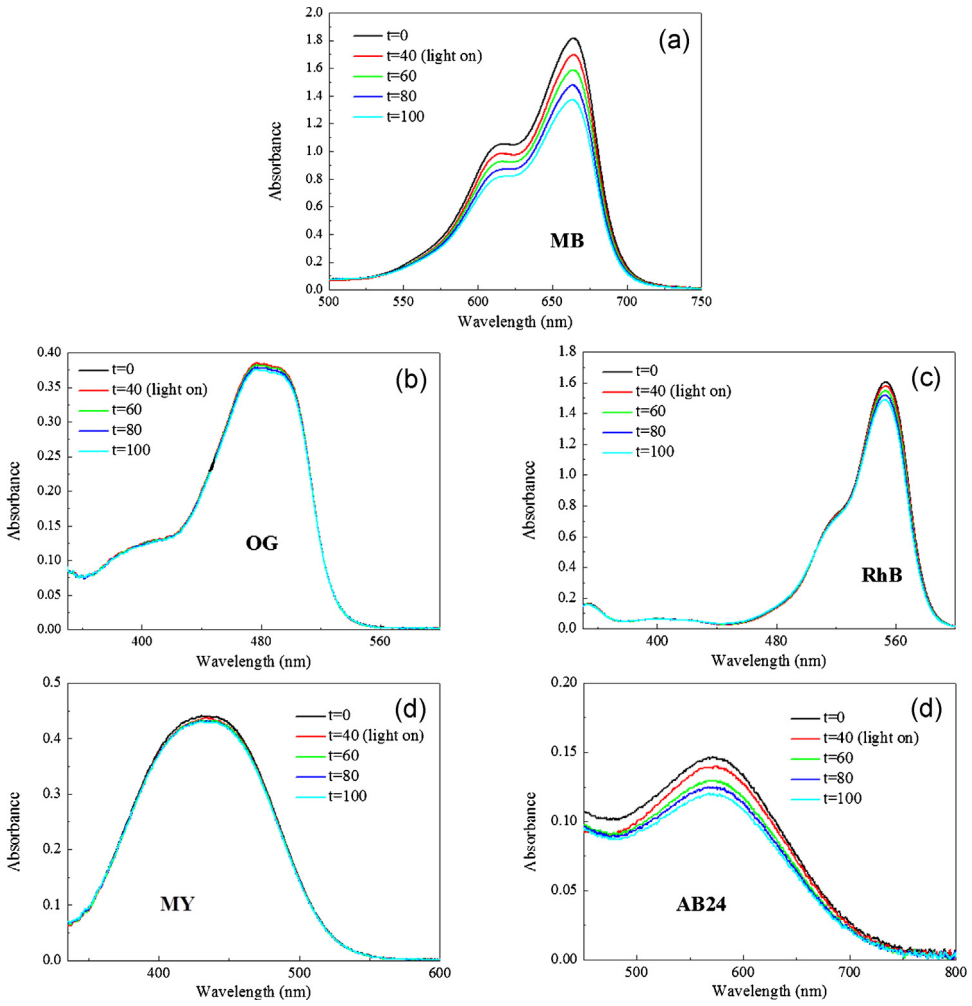

Fig. 5. The UV–Vis spectra of a newly prepared (a) MB, (b) OG, (c) RhB, (d) MY, and (e) AB24 solution. The dyes were adsorbed under dark on A-TiO_2 surface during the initial 40-min test and then dyes were decolorized under the simulated solar light irradiation for the following 60 min (i.e., *t* from 40 to 100 min).

for 30 min in order to effectively evaluate the difference in the adsorption ability of dyes on A-TiO_2. The adsorption contents of various dyes on A-TiO_2 are shown in Table 5. From this table, the order of dyes with respect to decreasing the adsorption percentage is: AB24 (14.57%) > MB (1.77%) > RhB (1.06%) > OG (0%) ≈ MY (0%), which strongly depends on the electrostatic interactions at the interface between A-TiO_2 and dye solution. From a comparison of Tables 4 and 5, the photocatalytic decoloration rate under the simulated solar light irradiation is directly proportional to the adsorption amount of dyes with the exception of AB24. However, the decoloration rate of RhB is expected to be about 17 times of MB and 24 times of AB24 on the basis of the photo-sensitizing enhancement mechanism. Accordingly, dye adsorption is considered to be the fundamental key of this photocatalytic degradation reaction since the contribution of the dye-sensitized current injected from the LUMO of RhB into A-TiO_2 to generate strong oxidants responsible for the photocatalytic decoloration of RhB is minor.

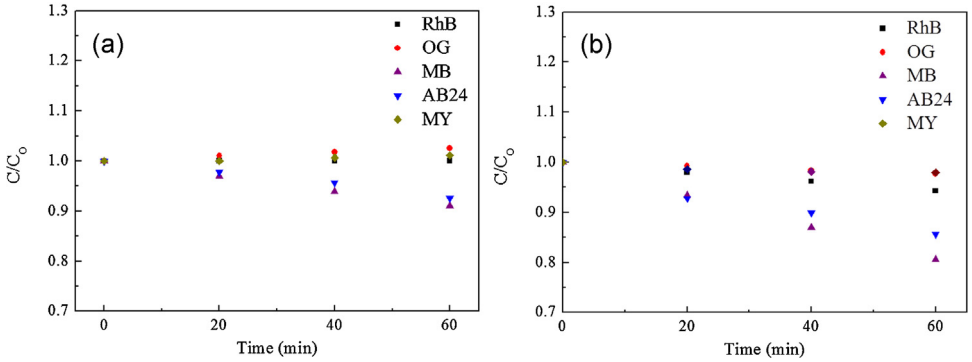

Fig. 6. The variance in C/C_0 against decoloration time for MB, OG, RhB, MY, and AB24 during (a) the photo-decoloration and (b) the photocatalytic decoloration on A-TiO_2 photo-anode under the simulated solar light irradiation.

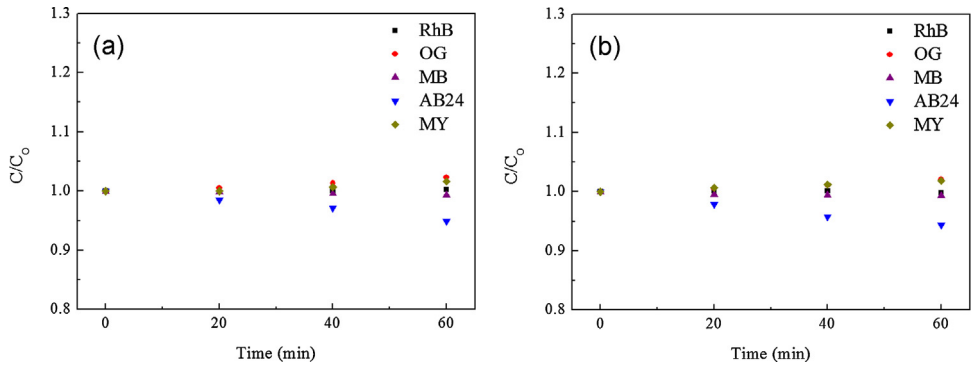

Fig. 7. The variance in C/C_0 against decoloration time for MB, OG, RhB, MY, and AB24 during (a) the photo-decoloration and (b) the photocatalytic decoloration on A-TiO_2 photo-anode under the Vis-light irradiation.

Note that the lower photocatalytic decoloration percentage of AB24 in comparison with MB seems in conflict with the above claim. This phenomenon, on the other hand, is attributable to three possible reasons. First, the higher adsorption content of AB24 leads to a higher shielding effect. Moreover, AB24 shows a higher ability of Vis-light absorption in comparison with MB, enhancing the shielding effect. Second, the adsorption amount of AB24 is expected to be too high to effectively generate highly oxidative species (e.g., $O_2^{-\bullet}$ and OH•) because the strong adsorption of AB24 molecules causes the loss in active sites for generating $O_2^{-\bullet}$ and/or OH•. Third, the desorption of certain intermediates (derived from the oxidation of adsorbed AB24) from the A-TiO_2 surface might be not easy, further inhibiting the generation of the highly oxidative species from the active sites of A-TiO_2.

Fig. 7(a) and (b) respectively shows the variation in C/C_0 of various dyes with respect to the decoloration time for photo-decoloration and photocatalytic decoloration by the A-TiO_2 photo-anode under the Vis-light irradiation. The quantitative data of the above two tests are shown in Table 4 for comparison purposes. From an examination of Tables 4 and 5, several features have to be described. First, based on the data of OG and MY, the visible light cannot drive the photocatalytic decoloration of dyes on A-TiO_2, reasonably due to the fact that A-TiO_2 is an UV-driven photocatalyst and that OG and MY do not adsorb on A-TiO_2. Second, AB24 can be easily decomposed by the photons of visible light, indicating its photochemical instability. Third, although AB24 and MB (minor amount) can be decomposed by the visible light, no significant contribution from the photocatalytic decoloration is found for both dyes under the Vis-light irradiation. This result is reasonably attributed to that the photo-excited electrons of MB and AB24 cannot be effectively injected from the LUMO of these dyes into the conduction band of A-TiO_2 to generate the oxidative species to decompose the dyes. The minor increase in the AB24 decoloration percentage (0.59%) via the photocatalytic route may be due to enhanced photo-decomposition of AB24 molecules adsorbed onto A-TiO_2 photo-anode although the exact reasons are unclear. Fourth, the contribution via the photo-sensitizing enhancement route (i.e., the dye-sensitized current injected from the LUMO of RhB into A-TiO_2 to generate strong oxidants) is only 0.19% which is smaller than that (0.59%) of the photocatalytic decoloration of AB24 under the Vis-light irradiation in Table 4.

Table 5
The adsorption percentages of MB, OG, RhB, MY and AB24 for 1 mg A-TiO_2 powders dispersed in a 20-mL solution containing 10 mg L^{-1} dye under stirring in darkness for 30 min.

Dye	Blank (without TiO_2) (%)	Adsorption percentage on TiO_2 (%)
MB	2.53	4.30
OG	0.00	0.00
RhB	1.07	2.13
MY	0.00	0.00
AB24	9.27	23.84

Based on the above results and discussion, the contribution of the dye-sensitized current injected from the LUMO of RhB into A-TiO_2 to generate strong oxidants responsible for the photocatalytic decoloration of RhB is negligible, which is attributable to two reasons (also see the modified scheme shown in Fig. 8). First, only a small amount of RhB molecules have been adsorbed onto A-TiO_2 when the test medium is an aqueous solution although the photo-excited electrons generated from the adsorbed RhB are able to be injected into the CB of A-TiO_2. The electron injection will result in the formation of positively charged RhB (denoted as RhB^+). However, these positively charged species cannot be regenerated through the redox reaction, $2RhB^+ + 3I^- \rightarrow 2RhB + I_3^-$, since there is no I_3^-/I^- couple in the dye-containing test solution. Accordingly, RhB^+ will decompose spontaneously into other organic species since RhB^+ should be very active. The above descriptions also imply that under the Vis-light illumination, the adsorbed RhB molecules will donate few photo-excited electrons to the A-TiO_2, leading to the low dye-sensitized current density (ca. 451.73 nA cm^{-2} from Table 3) because of the poor RhB adsorption in the aqueous media, although the above low RhB-sensitized current density on A-TiO_2 may be used to generate $O_2^{-\bullet}$ for dye decomposition. Second, if the adsorbed RhB^+ is stabilized on the A-TiO_2 surface, RhB^+ might trap the newly injected electrons from the other adsorbed RhB molecules (or the electrons photo-excited from A-TiO_2 under the simulated solar light irradiation). This effect is believed to reduce the generation of highly oxidative species (i.e., $O_2^{-\bullet}$ or OH•) on the A-TiO_2 surface, leading to a lower decoloration rate.

In summary, the adsorption content of dyes (i.e., the electrostatic interactions between dye in the waste influent and A-TiO_2)

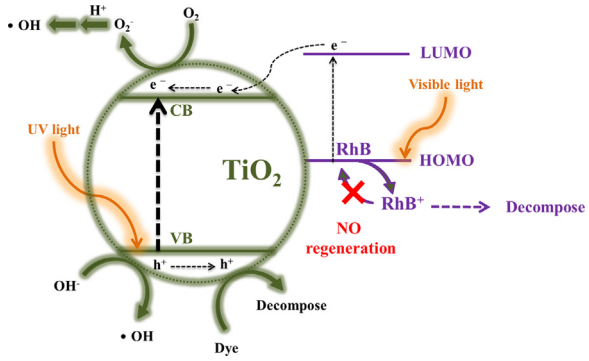

Fig. 8. The modified schematic mechanism illustrates the matched band position between the LUMO of RhB and CB of A-TiO_2. RhB is mainly decolorized by $O_2^{-\bullet}$, OH• generated via the photo-excited electron/hole pairs formed on A-TiO_2, and/or directly oxidized by the photo-excited holes on A-TiO_2 under the UV light illumination.

is concluded to be the key factor determining the photocatalytic decoloration rate of dyes on A-TiO_2 since dyes are mainly decolorized by $O_2^{-\bullet}$ and OH• generated via the photo-excited electron/hole pairs (and directly oxidized by the photo-excited holes) formed on A-TiO_2 by the UV light illumination. On the other hand, the shielding effect of adsorbed dye should decrease the generation of photo-excited electron/hole pairs. In addition, the adsorption of dyes may change the rate of $O_2^{-\bullet}$, OH• and photo-excited electron/hole pairs generation on the A-TiO_2 surface. Accordingly, there should be a compromise between the adsorption content of such photo-insensitive dyes (e.g., MB, OG, MY, and AB24 in this study) and the photocatalytic decoloration rate. As a result, too strong adsorption of dyes (e.g., AB24) reasonably leads to a lower decoloration rate because of the more significant light-shielding effect of dyes and the less effective generation of $O_2^{-\bullet}$ and OH• in comparison with those with a suitable adsorption property (e.g., MB).

4. Conclusions

From the *J–V* (photocurrent density against cell voltage) curves of DSSCs soaked with various dyes, RhB and N719 are effective photo-sensitizers converting photons into electrons which can be injected into the conduction band of A-TiO_2. However, MB, OG, MY, and AB24 cannot work as the photo-sensitizer on A-TiO_2 due to the unmatched band position between dyes and A-TiO_2, supported by the photo-electrochemical polarization curves obtained from the KCl + dye solutions. In the photocatalytic decoloration of MB, OG, RhB, MY, and AB24 on A-TiO_2 in aqueous media, the adsorption content of dyes on A-TiO_2 becomes the key factor determining the photocatalytic decoloration rate since dyes are mainly decolorized by $O_2^{-\bullet}$ and OH• generated via the photo-excited electron/hole pairs as well as by the photo-excited holes directly formed on A-TiO_2 by the UV light illumination. The contribution of dye-sensitizing currents on the photocatalytic decoloration of RhB is minor because the dye-sensitizing/electron-injection/dye-regeneration cycle cannot be completed in the degradation media while adsorbed RhB molecules should be unstable when their photo-generated electrons have been injected into the conduction band of A-TiO_2, probably leading to the decomposition of RhB^+.

Acknowledgements

The financial supports of this work, the National Science Council of ROC-Taiwan (NSC 101-2221-E-007-112-MY3), the Ministry of Economic Affairs of ROC-Taiwan (MEA 101-EC-17-A-08-S1-208), and the boost program from the LCERC of NTHU, are gratefully acknowledged.

References

[1] A. Fujishima, T.N. Rao, D.A. Tryk, J. Photochem. Photobiol., C 1 (2000) 1–21.
[2] W. Zhou, G. Du, P. Hu, Y. Yin, J. Li, J. Yu, G. Wang, J. Wang, H. Liu, J. Wang, H. Zhang, J. Hazard. Mater. 197 (2011) 19–25.
[3] Y.C. Hsiao, Y.H. Tseng, Micro Nano Lett. 5 (2010) 317–320.
[4] Y. Hou, J. Qu, X. Zhao, P. Lei, D. Wan, C.P. Huang, Sci. Total Environ. 407 (2009) 2431–2439.
[5] J.A. Rengifo-Herrera, E. Mielczarski, J. Mielczarski, N.C. Castillo, J. Kiwi, C. Pulgarin, Appl. Catal., B 84 (2008) 448–456.
[6] C.L. Cheng, W.C. Chu, D.S. Sun, Y.H. Tseng, H.C. Ho, J.B. Wang, P.H. Chung, J.H. Chen, P.J. Tsai, N.T. Lin, M.S. Yu, H.H. Chang, J. Biomed. Sci. 16 (2009) 7.
[7] W.C. Lin, C.H. Chen, H.Y. Tang, Y.C. Hsiao, J.R. Pan, C.C. Hu, C.P. Huang, Appl. Catal., B 140–141 (2013) 32–41.
[8] C. Chen, W. Cai, M. Long, B. Zhou, Y. Wu, D. Wu, Y. Feng, ACS Nano 4 (2010) 6425–6432.
[9] D. Su, J. Wang, Y. Tang, C. Liu, L. Liu, X. Han, Chem. Commun. 47 (2011) 4231–4233.
[10] M. Grätzel, Nature 414 (2001) 338–344.
[11] P. Chowdhury, J. Moreira, H. Gomaa, A.K. Ray, Ind. Eng. Chem. Res. 51 (2012) 4523–4532.
[12] R. Vinu, S. Polisetti, G. Madras, Chem. Eng. J. 165 (2010) 784–797.
[13] H. Chang, C.H. Chen, M.J. Kao, S.H. Chien, C.Y. Chou, Appl. Surf. Sci. 275 (2013) 252–257.
[14] A.H. Zyoud, N. Zaatar, I. Saadeddin, C. Ali, D. Park, G. Campet, H.S. Hilal, J. Hazard. Mater. 173 (2010) 318–325.
[15] A.L. Linsebigler, G. Lu, J.T. Yates Jr., Chem. Rev. 95 (1995) 735–758.
[16] H. Böttcher, B. Mahltig, J. Sarsour, T. Stegmaier, J. Sol–Gel Sci. Technol. 55 (2010) 177–185.
[17] A. Folli, U.H. Jakobsen, G.L. Guerrini, D.E. Macphee, J. Adv. Oxid. Technol. 12 (2009) 126–133.
[18] C.C. Yang, H.Q. Zhang, Y.R. Zheng, Curr. Appl. Phys. 11 (2011) S147–S153.
[19] Y. Lee, J. Chae, M. Kang, J. Ind. Eng. Chem. 16 (2010) 609–614.
[20] T.J. Savenije, A. Goossens, Phys. Rev. B: Condens. Matter 64 (2001) 115323.
[21] S.S. Mali, R.S. Devan, Y.R. Ma, C.A. Betty, P.N. Bhosale, R.P. Panmand, B.B. Kale, S.R. Jadkar, P.S. Patil, J.H. Kim, C.K. Hong, Electrochim. Acta 90 (2013) 666–672.
[22] Z. Zhang, Y. Yu, P. Wang, ACS Appl. Mater. Interfaces 4 (2012) 990–996.
[23] K. Kuribayashi, H. Iwata, F. Hirose, ESC Trans. 6 (2007) 15–19.